Electronic Supplementary Material (ESI) for Journal of Materials Chemistry B.
This journal is © The Royal Society of Chemistry 2019

Supporting Information

Controllable Growth of Ultrathin MnO_2 on Polydopamine Nanosphere as a Single Nanoplatform for MRI-Guided Synergistic Therapy of Tumor

Yanhong Sun[a,b], Hongda Chen[a,b], Guifeng Liu[*c], Lina Ma[*a], Zhenxin Wang[*a,b]

[a]State Key Laboratory of Electroanalytical Chemistry, Changchun Institute of Applied Chemistry, Chinese Academy of Sciences, Changchun, 130022, P. R. China.

[b]School of Applied Chemical Engineering, University of Science and Technology of China, Road Baohe District, Hefei, Anhui, 230026, P. R. China.

[c]Department of Radiology China-Japan Union Hospital of Jilin University, Xiantai Street, Changchun, 130033, P. R. China

Contents

1. **Additional Experimental Section**
2. **Additional Figures S1-S22**
3. **Additional Table S1**
4. **Additional References**

1. Additional Experimental Section

Materials. Dopamine Hydrochloride (99%) was purchased from Alfa Aesar (Ward Hill, USA). Methylene blue (MB) was obtained from Aladdin Reagent CO., Ltd. (Shanghai, China). The CCK-8 was obtained from Beijing Dingguo Biotechnology Ltd. (Beijing, China). $[Ru(dpp)_3]Cl_2$ (RDPP), calcein acetoxymethyl ester (Calcein AM) and propidium iodide (PI) were purchased from Dalian Meilun Biotechnology Ltd. (Dalian, China). 2,7-dichlorofluorescin diacetate (DCFH-DA) and 1, 3-diphenylisobenzofuran (DPBF) were obtained from Sigma-Aldrich CO. (MO, USA). The reduced glutathione assay kit was purchased from Nanjing Jiancheng Bioengineering Institute (Nanjing, China). The culture medium McCoy's 5A was purchased from Jiangsu KeyGEN BioTECH Co. Ltd. (Jiangsu, China). Fetal bovine serum (FBS) and trypsin cell detaching kit were purchased from Gibco Co. (New York, USA). HCT116 cell lines were purchased from Shanghai Cell Bank, CAS (Shanghai, China). The other reagents were obtained from Beijing Chemical Reagents Company (Beijing, China). BALB/c nude mice (female, 6~8 weeks old) with average bodyweight of 20 g were purchased from Vital River Ltd. (Beijing, China). Animal procedures were in agreement with the guidelines of the Regional Ethics Committee for Animal Experiments established by Jilin University Institutional Animal Care and Use. All chemicals were analytical grade and used as received without further purification. Milli-Q water (18.2 MΩ cm) was used in all experiments.

Characterization. The morphology of nanoparticles was recorded by a Hitachi H-600 electron microscope with an acceleration voltage of 100 kV (Hitachi Ltd, Japan). The Fourier transform infrared (FT-IR) spectra were recorded on a Bruker Vertex 70 spectrometer (Bruker, Germany). The powder X-ray diffraction (XRD) analysis was carried out on a D8 ADVANCE diffractometer (Bruker Co., Germany) using Cu Ka (0.15406 nm) radiation. The X-ray photoelectron spectroscopy (XPS) measurements were performed using a VG ESCALAB MKII spectrometer (VG Scientific Ltd, UK). Zeta potential and hydrodynamic size measurements were carried out on Malvern Zetasizer (Malvern Instruments Ltd, UK). The analysis of the elements was

performed by an ELAN 9000/DRC ICP-MS system (Perkin Elmer, USA). The CCK-8 assay was measured using a Versamax microplate reader (Bio-Tek Instruments, Inc., USA). The fluorescence images were performed with a reconstructive Ti-S fluorescent microscope (Nikon Co., Japan). The T_1-weighted MRI images were acquired using a Siemens 3 T MRI scanner (Magnetom Avanto, Siemens, Erlangen, Germany) with the following imaging parameters: repetition time, 613 ms; echo time, 8.4 ms; field of view, 102×72 mm; and slice thickness, 3.0 mm.

PDA nanoparticle Synthetic Methods. PDA nanoparticles were synthesized using the previously reported method.[1] In a typical synthesis of PDA nanoparticles with an average diameter of 60 nm, 4.5 mL of ammonia aqueous solution (NH_4OH, 28-30%) was mixed with 40 mL of ethanol and 90 mL of deionized water in a 250 mL round-bottom flask. After mild stirring at 30 °C for 30 min, 10 mL of deionized water containing 0.5 g dopamine hydrochloride was injected into the above mixture. The color of the solution immediately turned to pale yellow and gradually changed to dark brown. The reaction was allowed to proceed for 12 h. The PDA nanoparticles were obtained by centrifugation and washed with water for three times, and finally re-dispersed in distilled water.

Photothermal effect measurement. The aqueous PDA@ut-MnO_2/MB NF solution (0.1 mL) at different concentrations (0, 100, 200, 300, 400 μg mL^{-1}) was placed in 96-well plates. Every sample was irradiated under 808 nm laser with a power density of 1.5 W cm^{-2} for 480s or 400 μg mL^{-1} of PDA@ut-MnO_2/MB solution irradiated with 808 nm laser at different power densities (1.0, 1.3, and 1.5 W cm^{-2}), and the temperature was recorded every 20 s by an infrared camera. The photostability of PDA@ut-MnO_2/MB was measured by cycle irradiation. The aqueous PDA@ut-MnO_2/MB solution (400 μg mL^{-1}) was exposed to an 808 nm laser with a power density of 1.5 W cm^{-2} for 480 s, then, the laser was turned off, and the solution was cooled down naturally. This cycle was repeated 5 times and the temperature was recorded using the infrared camera.

Cell Culture and Cytotoxicity Assay of PDA@ut-MnO_2/MB. The human colon

cancer cell line HCT116 cells were cultured with 100 μL of fresh culture medium (fresh McCoy's 5A supplemented with 10% FBS and 100 U mL^{-1} penicillin-streptomycin) in 96 well microtiter plate (1×10^4 cells per well) under a humidified 5% CO_2 at 37 ºC for 24 h. After washed with 100 μL PBS (3 times), fresh culture medium (100 μL) with various concentrations (0, 50, 100, 300 and 400 μg mL^{-1}) of PDA@ut-MnO_2/MB NFs were added and incubated at same conditions for another 24 h, respectively. Subsequently, the cells were washed with 100 μL PBS (3 times), and then 100 μL medium with CCK-8 was added into each well and incubated for another 2 h. The absorption of each well was read at 450 nm. The relative cell viabilities (%) were calculated by using the optical den
sities with respect to the control value.

Endocytosis of PDA@ut-MnO_2/MB. The HCT116 cells were seeded in a 96-well plate for 24 h. Then the cells were incubated with PDA@ut-MnO_2/MB NFs (300 μg mL^{-1}) and free MB (11 μg mL^{-1}) for another 24 h，respectively. After each well was washed with PBS for three times, fluorescence of MB within cells were captured by fluorescent microscope using an excitation of 633 nm and an emission of 650 - 700 nm.

***In Vitro* Photodynamic/Photothermal Therapy Effect.** The HCT116 cells were seeded in a 96-well plate for 24 h, and then incubated with different concentrations of PDA@ut-MnO_2/MB NFs (50, 100, 200, 300 and 400 μg mL^{-1}). After incubation for 24 h, the cells were washed with PBS (0.1 mL, three times). For PDT, 100 μL fresh medium was added into each well and then irradiated with 650 nm laser (50 mW cm^{-2}) for 10 min. For PTT, the cells were irradiated with 808 nm laser (1.5 W cm^{-2}) for 8 min. After laser irradiation, the cells were incubated for another 24 h, and the cell viabilities were evaluated by CCK-8 assay (2 h) and calcein acetoxymethyl ester (Calcein AM)/propidium iodide (PI) co-staining (20 min), respectively. The normal cultured cells were used as control samples.

***In Vivo* Toxicology Analysis.** After 24h treatment, tmor-bearing mice were sacrificed and the tumor tissues were dissected for hematoxylin and eosin (H&E) staining. After

30 days post-injection of PDA@ut-MnO_2/MB NFs, healthy mice were sacrificed and the organs including heart, spleen, liver, lung, kidney and tumors were dissected for hematoxylin and eosin (H&E) staining. For blood analysis, healthy mice were intravenously injected with a single dose of PDA@ut-MnO_2/MB NFs (10 mg kg^{-1}). Untreated healthy mice were used as the control. After 30 days post-injection, the bloods were extracted and analyzed by blood parameters assay.

2. Additional Figures S1-S22.

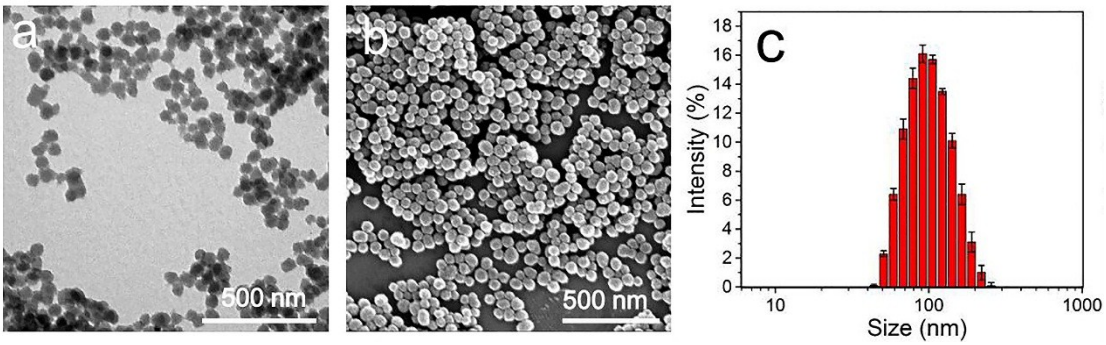

Figure S1. (a) TEM and (b) SEM micrographs of PDA nanoparticles, and (c) the hydrodynamic diameter of PDA nanoparticles in H_2O.

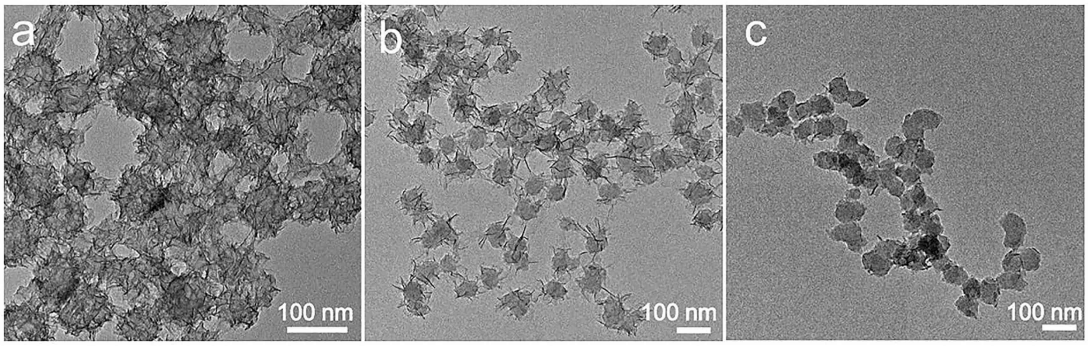

Figure S2. TEM micrographs of PDA@ut-MnO_2 NFs, which were prepared under different mass ratios of $KMnO_4$ to PDA nanoparticle ((a) 1:1; (b) 1:2; and (c) 1:4), respectively.

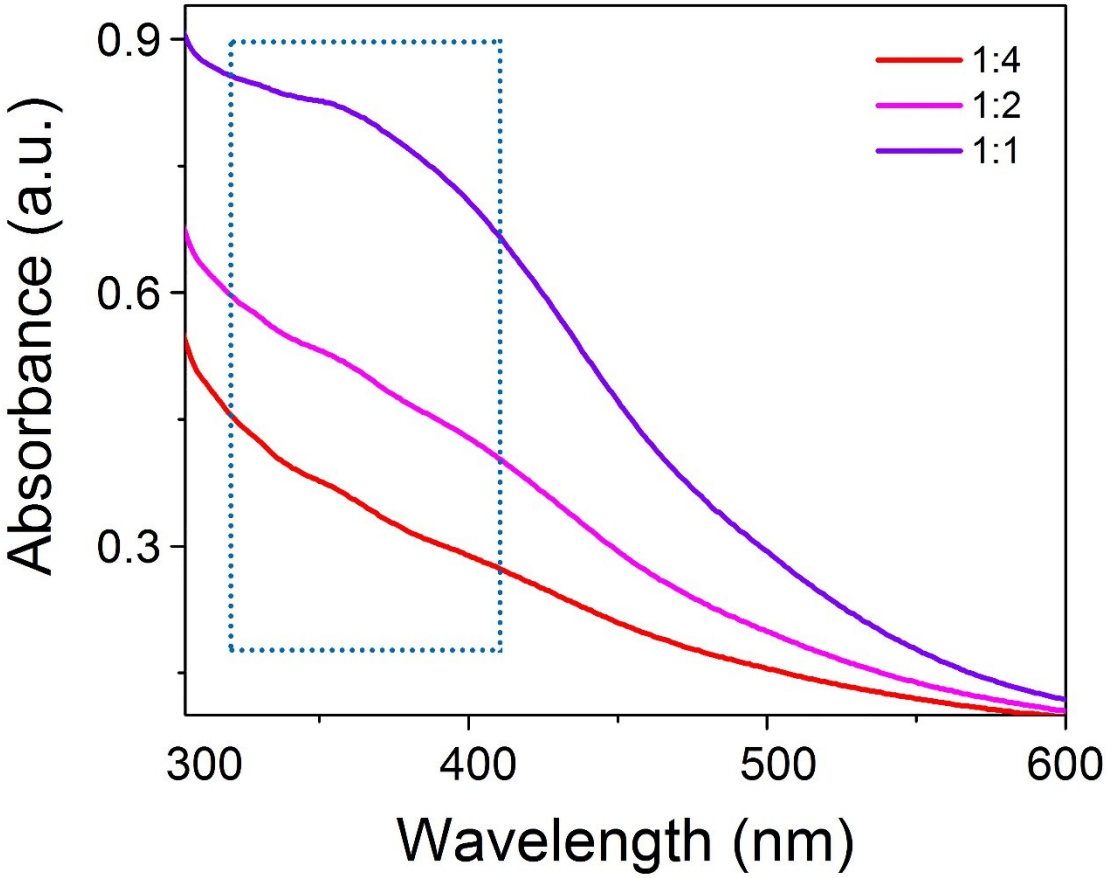

Figure S3. The UV -Vis spectra of PDA@ut-MnO_2 NFs, which were prepared under different mass ratios of $KMnO_4$ to PDA nanoparticle ((a) 1:1; (b) 1:2; and (c) 1:4, respectively.)

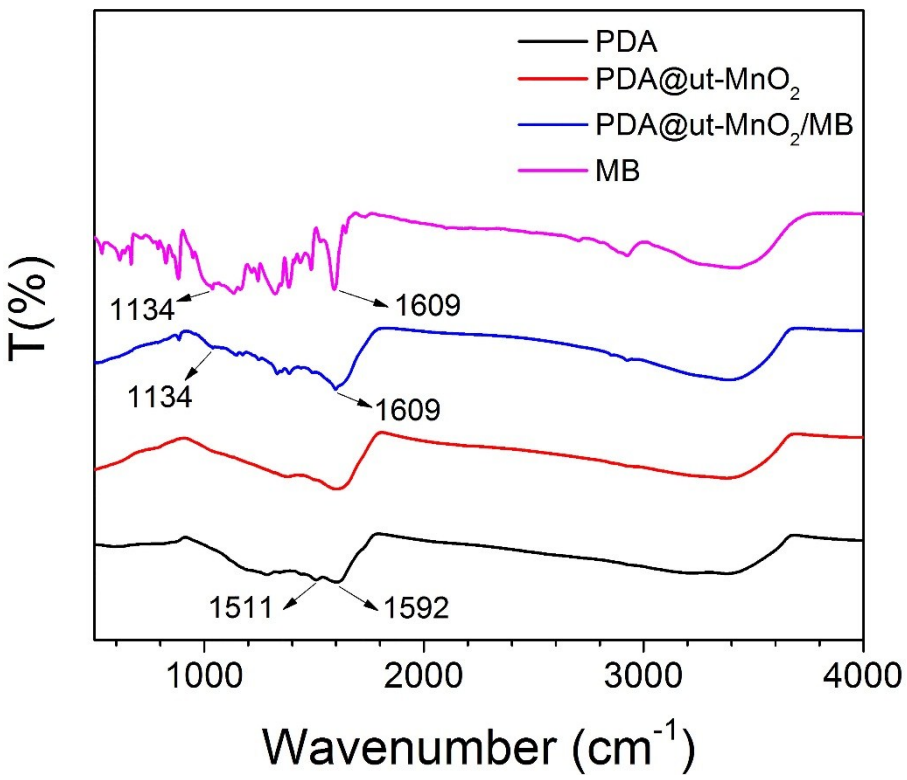

Figure S4. FTIR spectra of PDA nanoparticles, PDA@ut-MnO_2 NFs, PDA@ut-MnO_2/MB NFs and MB, respectively.

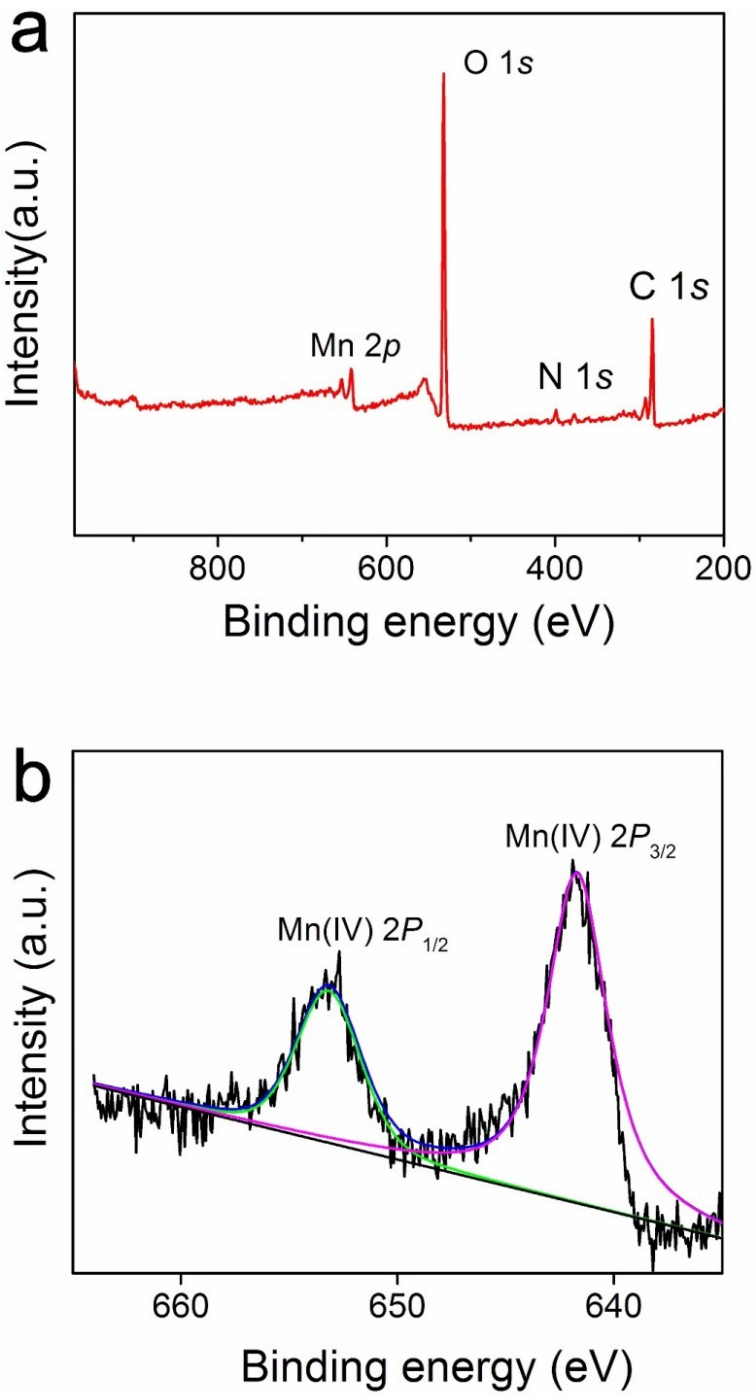

Figure S5. XPS spectra of (a) the as-synthesized PDA@ut-MnO_2 NFs and (b) Mn 2*p* level of PDA@ut-MnO_2 NFs.

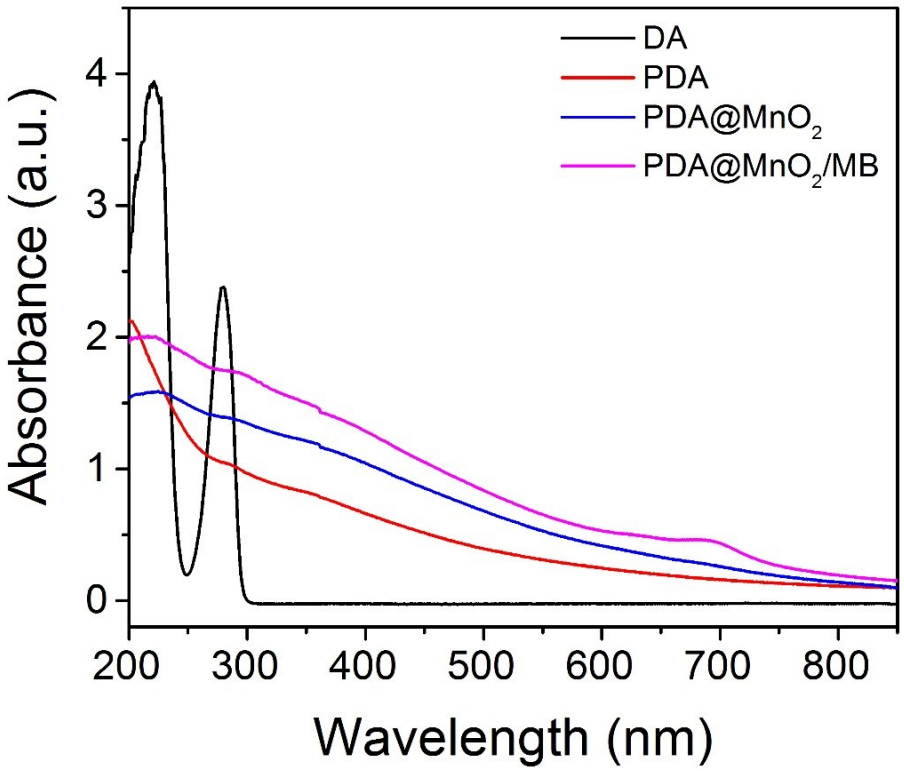

Figure S6. The UV -Vis spectra of DA monomers, PDA nanoparticles, PDA@ut-MnO_2 NFs and PDA@ut-MnO_2/MB NFs.

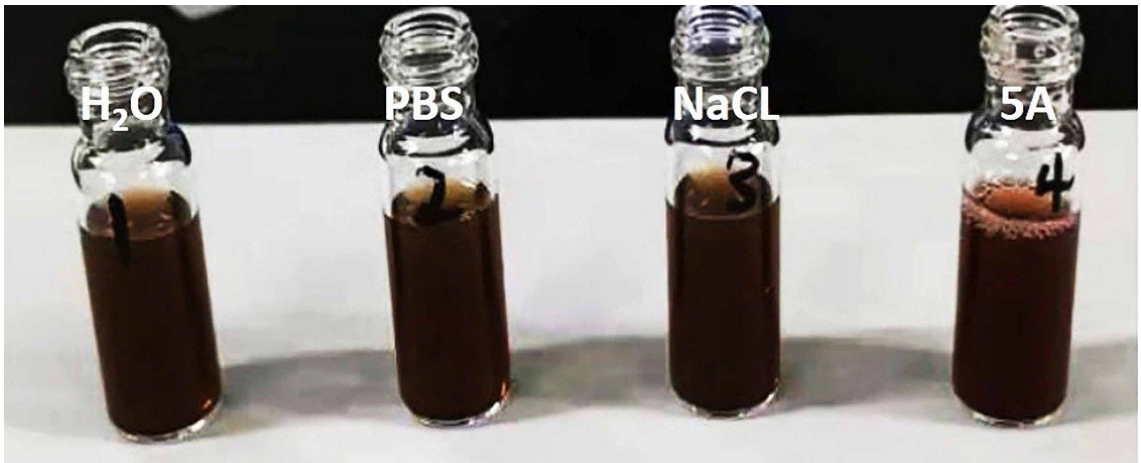

Figure S7. Dispersibilities of PDA@ut-MnO_2 NFs in H_2O, PBS, NaCl and complete culture medium (5A, McCoy's 5A medium plus 10% fetal bovine serum (FBS)).

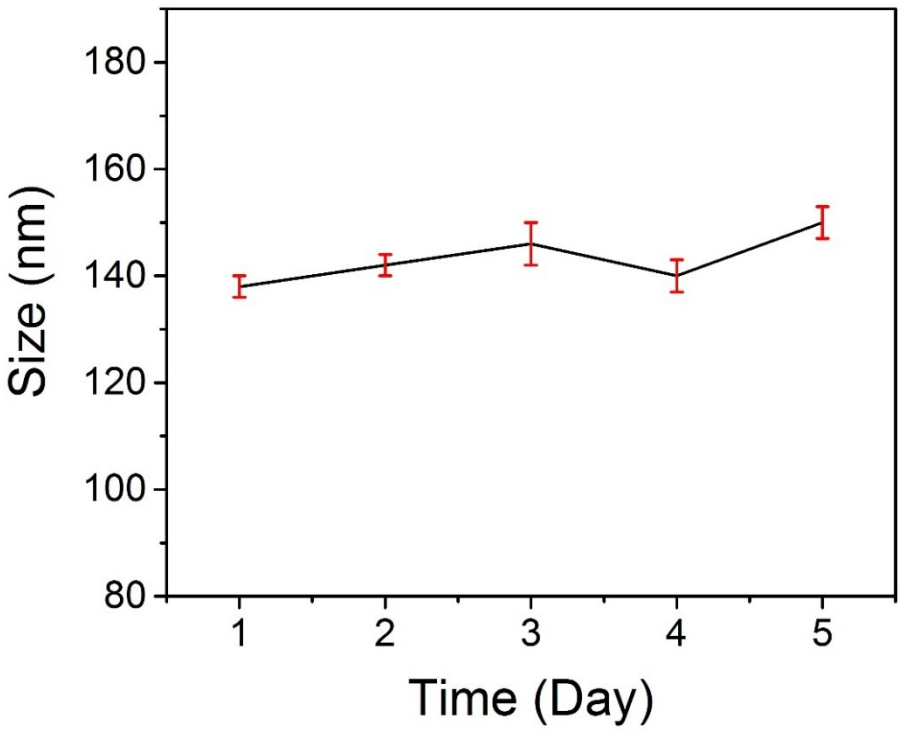

Figure S8. The hydrodynamic diameter of PDA@ut-MnO_2 NFs as a function of incubation time. The PDA@ut-MnO_2 NFs were dispersed in complete culture medium (5A, McCoy's 5A medium plus 10% fetal bovine serum (FBS)).

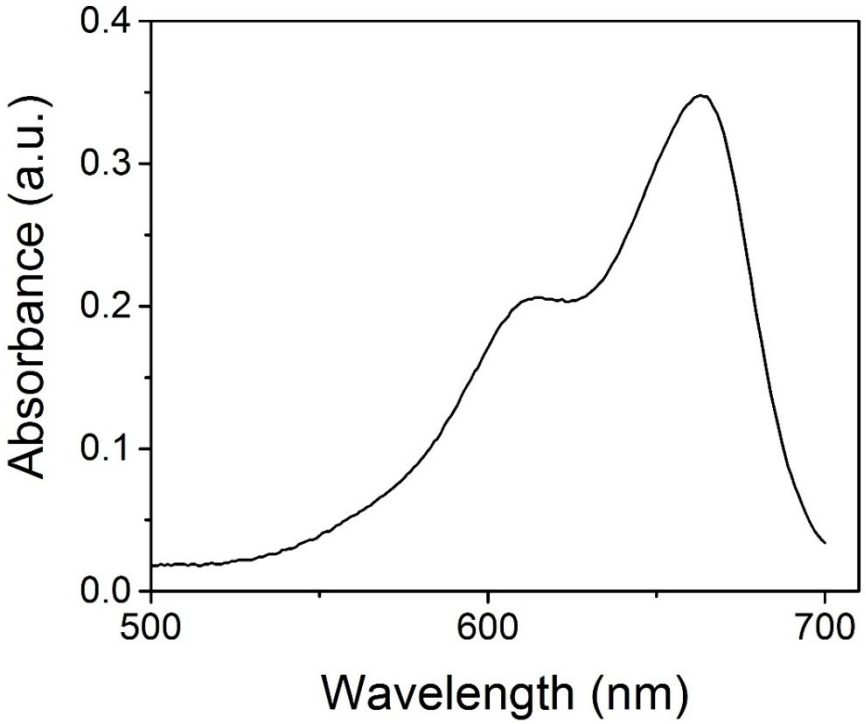

Figure S9. UV-Vis absorption spectrum of MB.

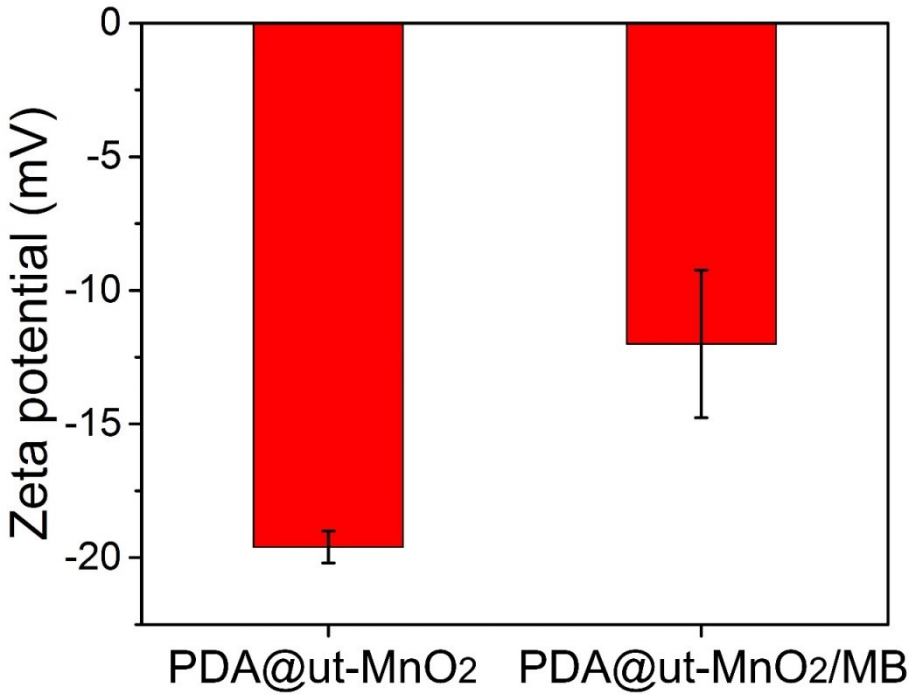

Figure S10. Zeta potentials of PDA@ut-MnO_2 NFs and PDA@ut-MnO_2/MB NFs.

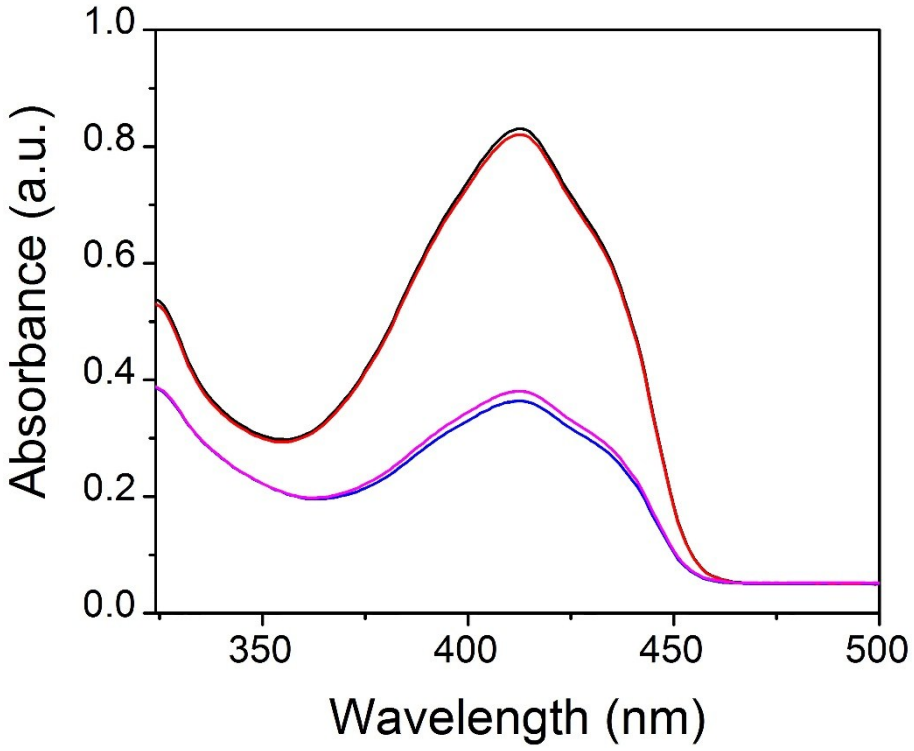

Figure S11. The UV-Vis spectra of DPBF in absence of PDA@ut-MnO_2/MB in pH 6.5 PBS with 300 μmol L^{-1} H_2O_2 under 650 nm laser irradiation for 10 min (black line), in presence of PDA@ut-MnO_2/MB in pH 7.4 PBS (red line), in presence of PDA@ut-MnO_2/MB PBS in pH 6.5 PBS with 300 μmol L^{-1} H_2O_2 for 12h (pink line) under 650 nm laser irradiation for 10 min, and in the presence of PDA@ut-MnO_2/MB in pH 7.4 PBS with 650 nm laser irradiation for 12h (blue line), respectively.

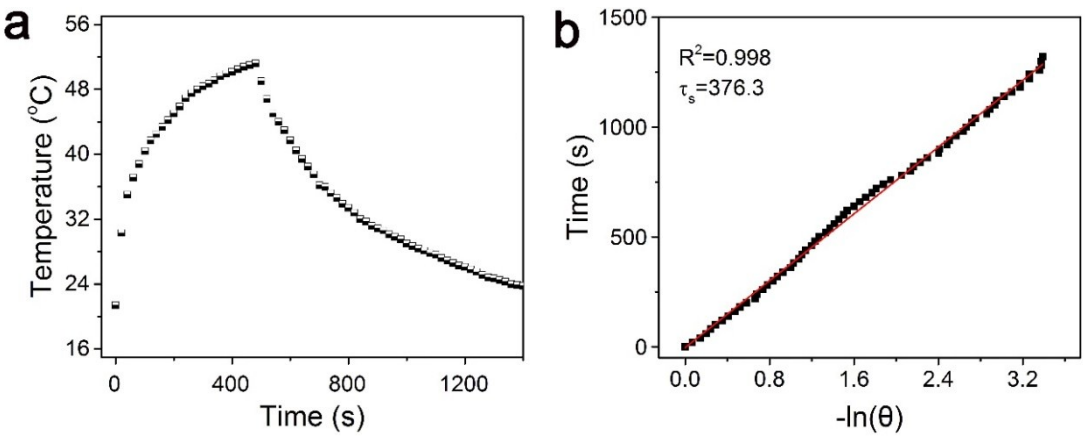

Figure S12. (a) Heating and cooling curve of PDA@ut-MnO_2/MB NFs (400 μg mL^{-1}) under irradiation with 808 nm NIR laser (1.5 W cm^{-2}). (b) Linear time data versus -lnθ obtained from the cooling period.

The photothermal conversion efficiency (η) of PDA@ut-MnO_2/MB NFs can be calculated by following equations:

$\eta = [hS (T_{max} - T_{surr}) - Q_{Dis}] / [I(1 - 10^{-A_{808}})] \times 100\ \%$

$hS = (\Sigma m_i C_{p,i})/\tau_s$

$t = \tau_s \times (-\ln\theta)$

$\theta = (T - T_{surr})/(T_{max} - T_{surr})$

To examine the photothermal conversion efficiency of PDA@ut-MnO_2/MB solution, PDA@ut-MnO_2/MB solution was irradiated with an 808 nm laser (1.5 W cm^{-2}) in a quartz cuvette for 480 s, (the distance between the liquid level and the laser head is 1.0 cm), and then the temperature was lowered by nature cooling. Subsequently, 1 mL of deionized water was measured in the same way. Where h is heat transfer coefficient, S is irradiated area, and T_{max} is the equilibrium temperature, T_{surr} is ambient temperature of the surroundings. The Q_{Dis} expresses the heat from light absorbed by the quartz sample cell itself, I is the laser power density, A is the absorbance of PDA@ut-MnO_2/MB NFs at 808 nm, m is the mass of sample, C_p is the thermal capacity of sample, t is cooling time after irradiation, and τ_s is the sample system time constant. The τ_s is 376.3 s obtained by Figure S9, hS is calculated to be 16.09 mW/°C, and the value of T_{max} - T_{surr} is 29.8 °C. So the photothermal conversion efficiency (η) of PDA@ut-MnO_2/MB NFs is calculated to be 28.75 %.

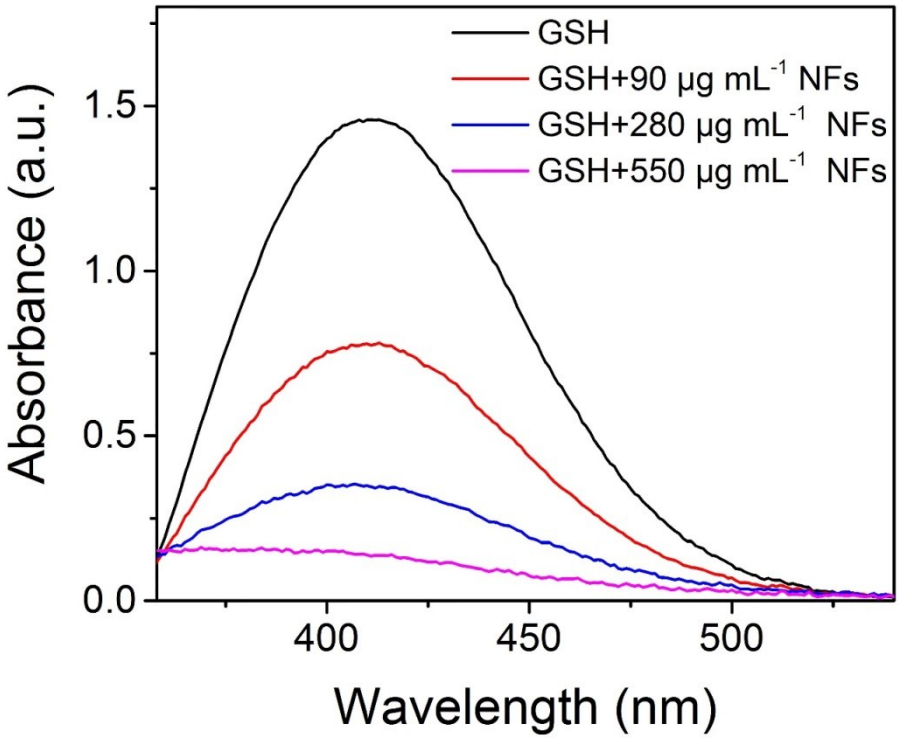

Figure S13. GSH depletion with different concentrations of PDA@ut-MnO_2/MB NFs (0, 90, 280 and 550 μg mL^{-1}). The concentration of GSH is 125 μmol L^{-1}. The reaction mixtures were incubated for 1 h.

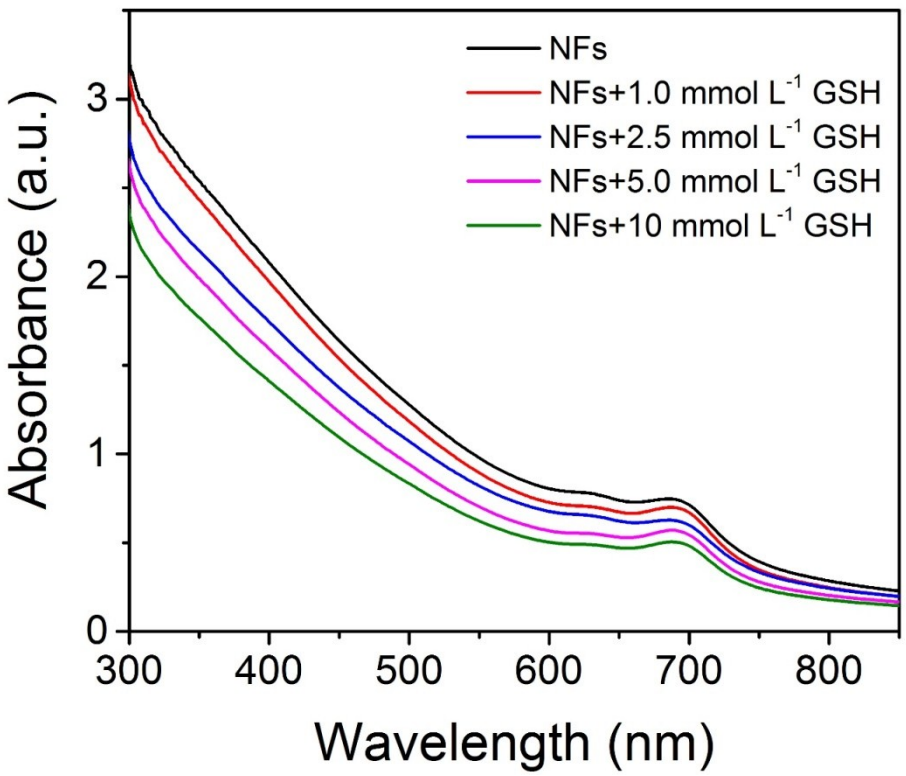

Figure S14. The UV-Vis spectra of PDA@ut-MnO_2/MB NFs after reacting with different concentrations of GSH (0, 1, 2.5, 5 and 10 mmol L^{-1}). The concentration of PDA@ut-MnO_2/MB NFs is 500 μg mL^{-1}. The reaction mixtures were incubated for 15 min.

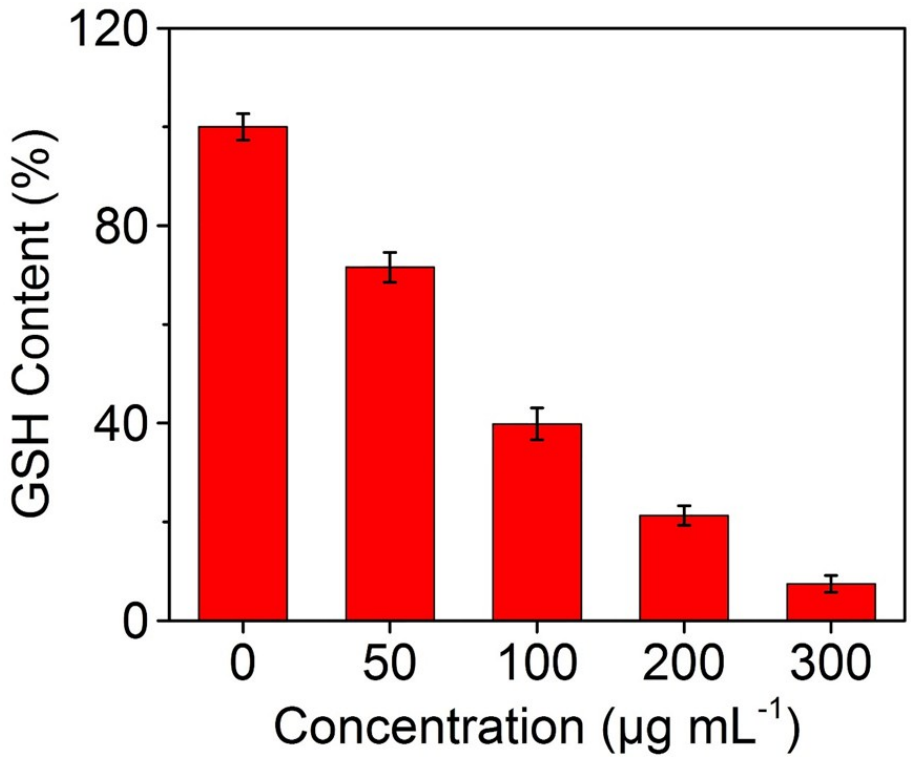

Figure S15. Intracellular GSH depletion with different concentrations of PDA@ut-MnO_2/MB NFs (0, 50, 100, 200 and 300 μg mL^{-1}).

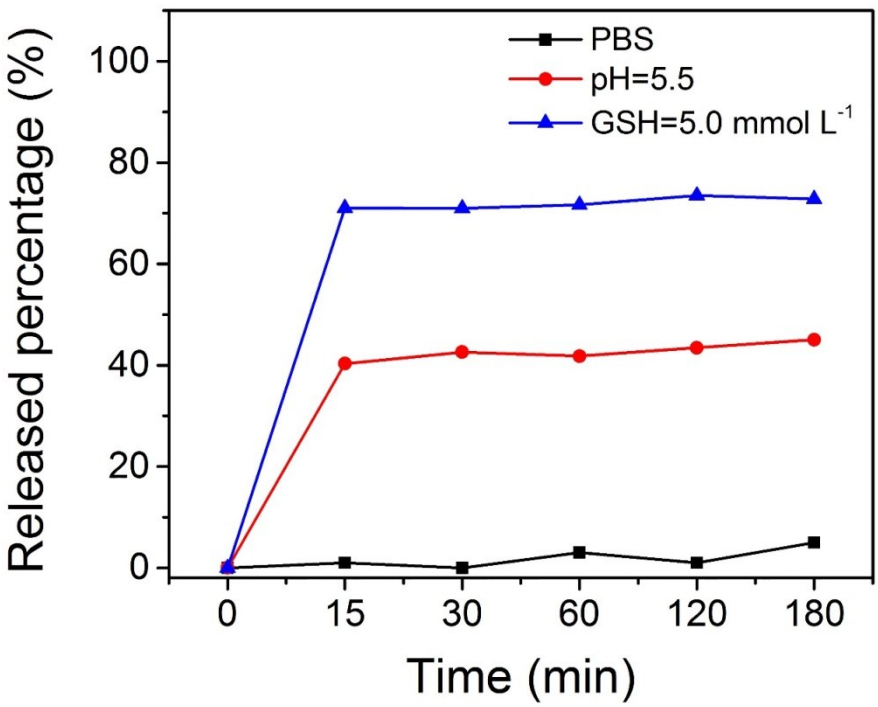

Figure S16. The percentage of released Mn^{2+} from PDA@ut-MnO_2/MB NFs under different conditions as a function of time.

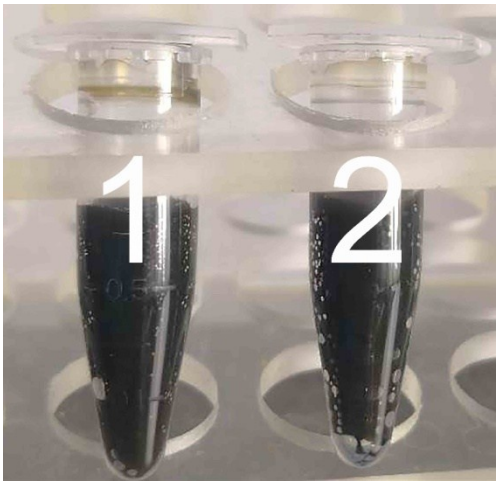

Figure S17. The digital photos of PDA@ut-MnO_2/MB NFs incubated in PBS (pH 6.5, containing 0.5 mmol L^{-1} H_2O_2) for 15 min without (1) or with 808 nm NIR laser irradiation for 8 min (2).

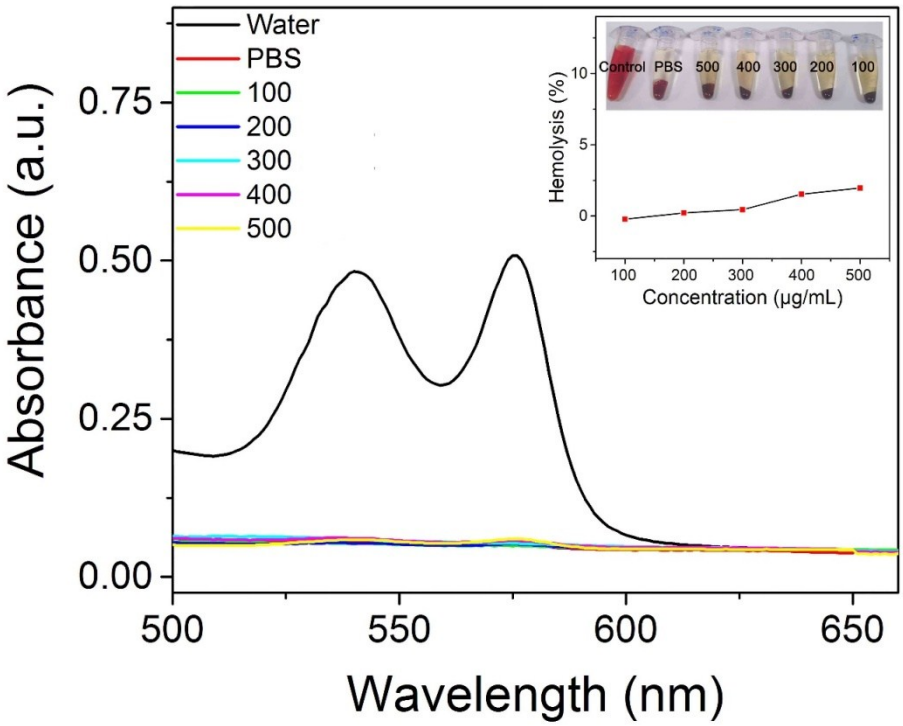

Figure S18. Hemolysis assay of PDA@ut-MnO_2/MB NFs. The PBS is used as negative control while H_2O is used as positive control, respectively. Inset illustrates the hemolysis percentage with different concentrations of NFs (100, 200, 300, 400 and 500 μg mL^{-1}).

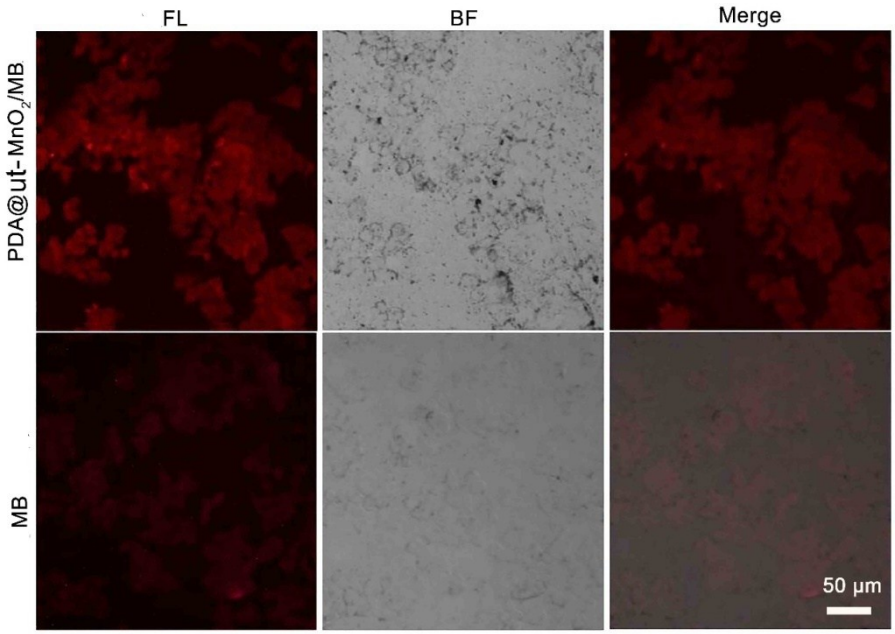

Figure S19. Fluorescence images (MB fluorescence channel images (FL), bright field images (BF) and merging images (merge)) of HCT116 cells treated with 300 μg mL^{-1} PDA@ut-MnO_2/MB NFs and 11 μg mL^{-1} free MB. The amount of MB on PDA@ut-MnO_2/MB NFs is equal to that of free MB.

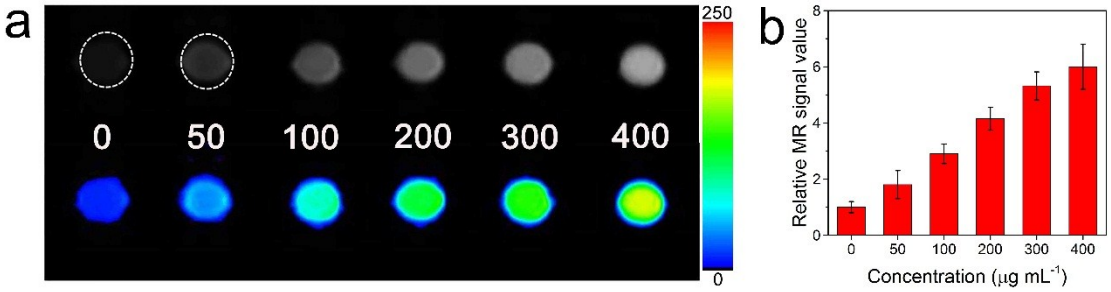

Figure S20. (a) MR images of PDA@ut-MnO_2/MB NF-stained HTC116 cells. (b) The relative MR signal values of PDA@ut-MnO_2/MB NF stained HCT116 cells. The cells were co-cultured with various concentrations of PDA@ut-MnO_2/MB NFs (0, 50, 100, 200, 300 and 400 μg mL^{-1}), respectively.

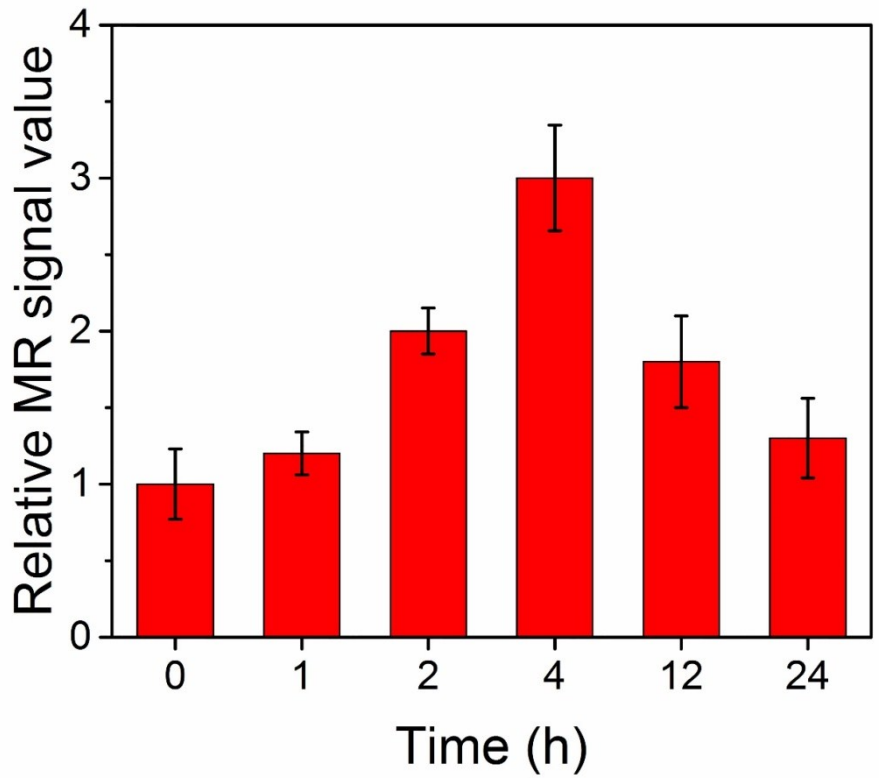

Figure S21. Relative MR signal value of tumor after intravenous injection of PDA@ut-MnO_2/MB NFs at different time intervals (0, 1, 2, 4, 12 and 24 h).

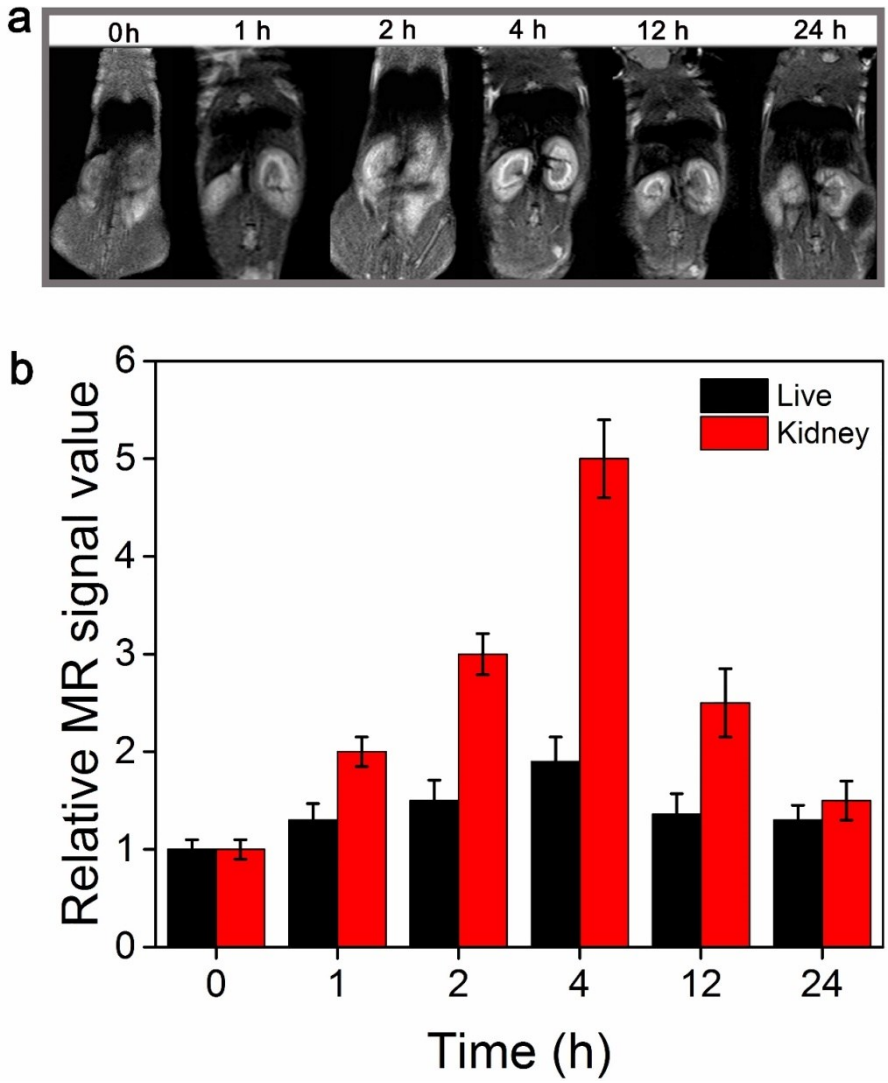

Figure S22. (a) *In vivo* T_1-weighted MR images (longitudinal section) of mice after intravenous injection of PDA@ut-MnO_2/MB NFs at different time intervals (0, 1, 2, 4, 12 and 24 h). (b) Relative MR signal value of Live and Kidney after intravenous injection of PDA@ut-MnO_2/MB NFs at different time intervals (0, 1, 2, 4, 12 and 24 h).

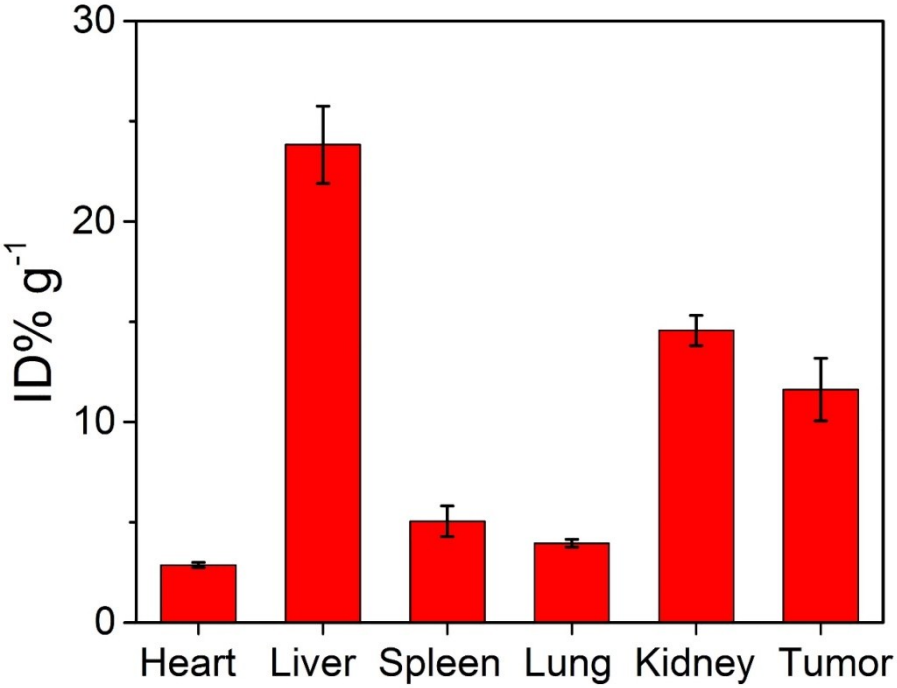

Figure S23. ICP-AES analysis of Mn element in major organs of HCT116 tumor-bearing mice at 4 h post injection of PDA@ut-MnO_2/MB NFs.

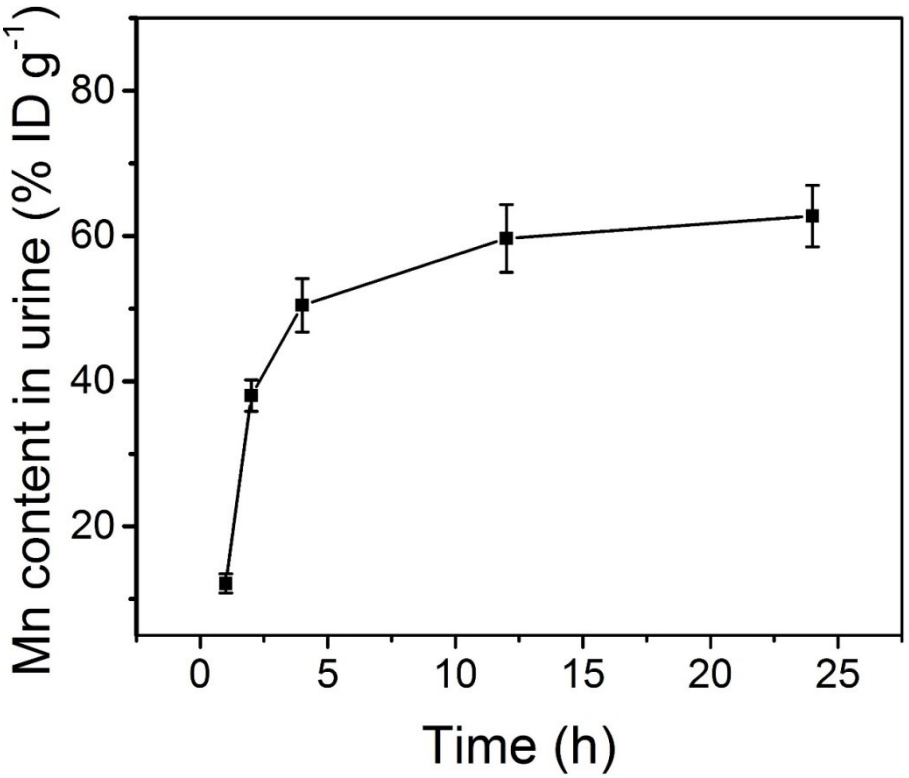

Figure S24. Total amounts of PDA@ut-MnO_2/MB NFs in mouse urine as a function of post-injection time.

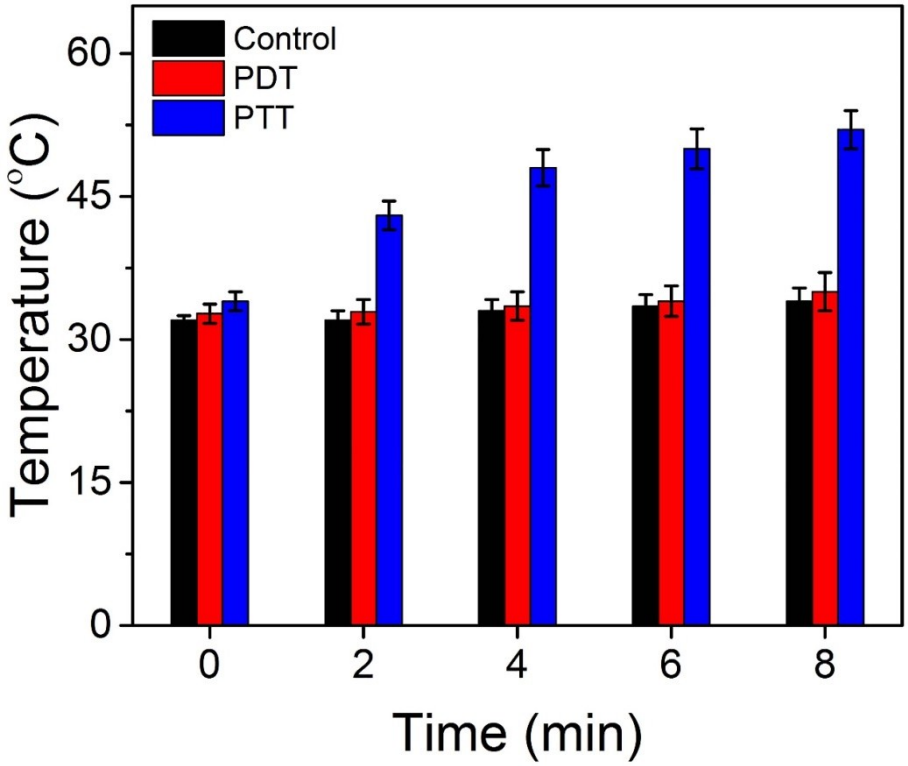

Figure S25. The temperature elevation of tumor site with different treatment at 4 h post-injection of PDA@ut-MnO_2/MB NFs.

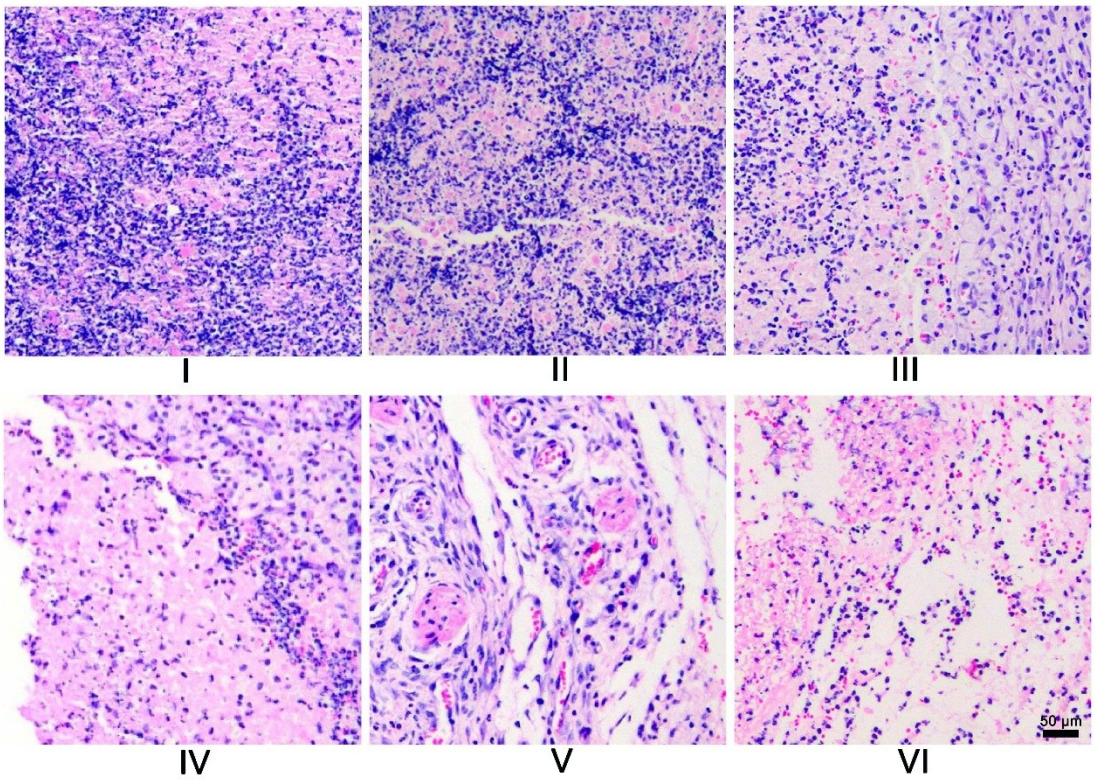

Figure S26. H&E staining of tumor slides from HCT116 tumor-bearing mice at 24 h post-treatment.

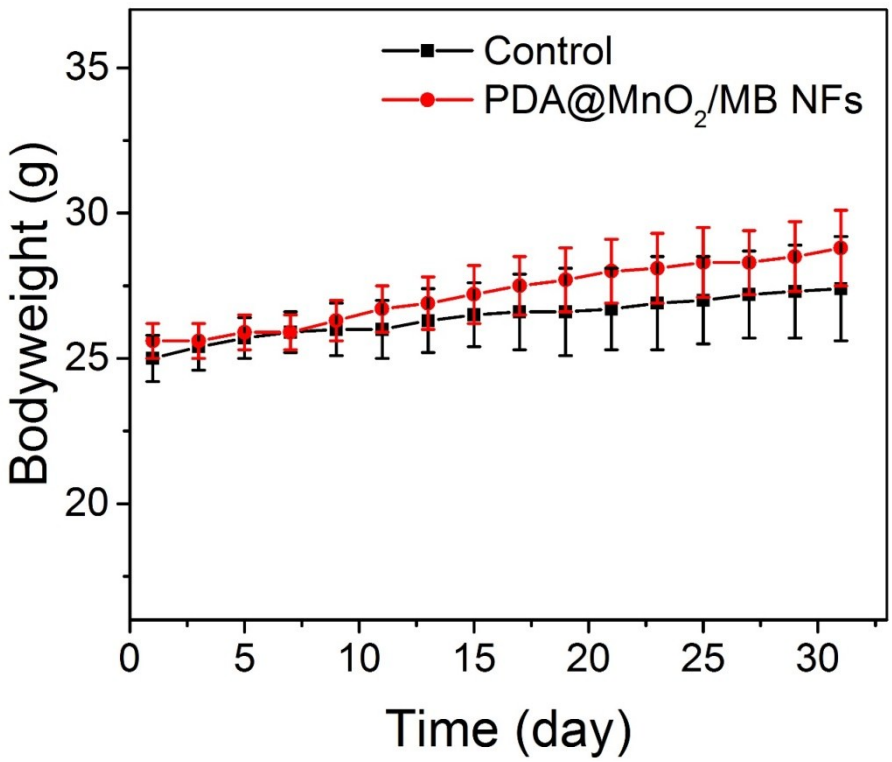

Figure S27. Bodyweight curves of health mice treated with PBS and PDA@ut-MnO_2/MB NFs, respectively.

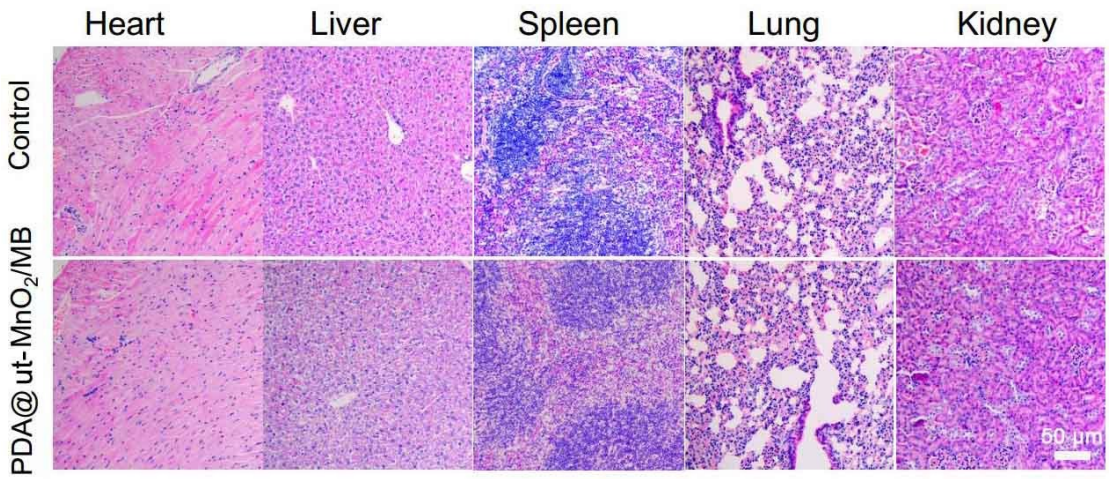

Figure S28. H&E staining of major organs from health mice treated with PDA@ut-MnO_2/MB NFs and normal reared mice (control), respectively.

Table S1 Hematology analysis of health mice treated with PDA@ut-MnO_2/MB NFs or normal reared mice (control).

Hematological	Units	Control	Treatment
WBC	$\times 10^9$/L	10.98	11.41
RBC	$\times 10^{12}$/L	10.22	10.75
HGB	g/L	161.21	169.20
MCV	fL	54.25	51.90
MCH	pg	14.52	15.67
MCHC	g/L	336.55	345.24
PLT	$\times 10^9$/L	960.46	950.02
PDW	fL	9.50	10.40

4. Additional Reference

S1. Liu, Y. L.; Ai, K. L.; Liu, J. H.; Deng, M.; He, Y. Y.; Lu, L. H. Dopamine-Melanin Colloidal Nanospheres: An Efficient Near-Infrared Photothermal Therapeutic Agent for In Vivo Cancer Therapy. *Adv. Mater.* **2013**, *25* (9), 1353-1359.